Intercoupling Suppression of Very Closely Spaced MIMO Antenna Based on Current Cancellation Method

ZHONGHONG DU[1], **XIAOHUI ZHANG**[1], **PEIYU QIN**[1,2],
YURONG PU[1], **(Member, IEEE), AND XIAOLI XI**[1], **(Member, IEEE)**
[1]Institute of Advanced Navigation and Electromagnetics, Xi'an University of Technology, Xi'an 710048, China
[2]Department of Electronic and Electrical Engineering, Brunel University London, UB8 3PH London, U.K.

Corresponding author: Xiaohui Zhang (xhzhang@xaut.edu.cn)

ABSTRACT Herein, a high isolation multiple-input−multiple-output (MIMO) antenna with a very close array element spacing, is proposed. By loading a pair of L-shaped parasitic stubs on the antenna feeder, the impedance matching bandwidth of the antenna is significantly improved. Furthermore, since the $\lambda/2$ microstrip line can make the signal through it produce 180°phase transformation at the resonant frequency. A dielectric wall decoupling structure with$\lambda/2$metal microstrip lines etched on both sides of the substrate is designed, and its profile height is 1.3 mm $(0.022\lambda_0)$.When the antenna element edge-to-edge distance is only 1mm $(0.017\lambda_0)$, the isolation of the MIMO antenna at the resonant frequency of 5.37 GHz is improved from 8.5 dB to 60 dB by introducing the dielectric wall decoupling structure. Finally, the close-spacing MIMO antennas using current cancellation method are compared, and the results show that the proposed decoupling structure is simple and has great versatility and extensibility.

INDEX TERMS Current cancellation method, high isolation, multiple input multiple output (MIMO) antenna.

I. INTRODUCTION

Massive multiple-input−multiple-output (M-MIMO) technology has become one of the key technologies in fifth-generation (5G) wireless communication systems [1], [2]. With the increasing number of MIMO antenna elements and the increasing miniaturization of equipment, the mutual coupling between compact MIMO antenna elements is becoming more and more serious [3]. Therefore, it is urgent to develop a reasonable decoupling structure when the distance between MIMO antenna array elements is very close. As reported in previous studies, the isolation between the antenna elements in the M-MIMO antenna array is greater than at least 25 dB [4].

In recent years, researchers have made significant efforts have been made to address the strong coupling problem of MIMO antenna with a very small array element spacing [5]. For example, methods to improve isolation by reducing or counteracting the original coupling field or coupling

The associate editor coordinating the review of this manuscript and approving it for publication was Tutku Karacolak[ID].

current are reported. Common decoupling structures include defected ground structure (DGS) [6], [7], [8], electromagnetic band-gap (EBG) structure [9], [10], parasitic resonance structure [11], [12], [13], [14], [15], neutralization lines [16], [17], [18], decoupling networks [19], [20], [21] and polarization-conversion decoupling [22], [23].

The coupling field/current cancellation method refers to artificially creating an additional coupling path with equal amplitude and opposite phase to improve the isolation between two antenna elements. In [13], a simple microstrip U-section was added between the antenna elements to form an indirect coupling path for field cancellation. However, this microstrip structure occupied a large amount of antenna element spacing. In [15], a three-port high isolation monopole MIMO antenna operating at 3.5 GHz is proposed. High isolation is achieved by introducing two reactive load dummy elements between the antennas. The results show that the isolation is better than −30 dB within the band of interest. In another study [23], a decoupling structure of the polarized conversion surface coplanar with the antenna was reported, which achieved coupling suppression above 19.6 dB

by changing the polarization direction of the coupling field, the array element spacing of the MIMO antenna was about 9 mm ($0.174\lambda_0$).

Furthermore, metamaterials and metasurfaces are also widely used for MIMO antenna coupling suppression because of their good electromagnetic field control ability [24], [25], [26], [27], [28], [29], [30]. In [26], Haoze Luan utilized a simple ring slot metasurface to enhance the isolation of the E/H-plane coupled patch antennas. By suppressing surface waves and partially changing the coupling mode, the coupling suppression of the MIMO antenna exceeded 40 dB. However, the use of metasurface decoupling can significantly increase the profile height of the antenna, which is not conducive to the miniaturization of the array antenna.

Recently, some self-decoupling methods using the characteristics of the antenna itself have been proposed, such as weak field coupling [31] and mode cancellation [32], [33], [34], [35], [36]. The self-decoupling technology employs unique antenna elements to reduce mutual coupling without introducing an additional decoupling structure and therefore has a subtle antenna structure. Although self-decoupling method is novel and effective, it lacks system design criteria and needs to continuously optimize the structure and layout of the antenna elements. For instance, in [31], the feed structure of the microstrip patch antenna is improved, and the coupling field from the feeding structure is utilized to counteract the coupling from the radiation patch, so that the electric field around the coupled patch antenna is very weak and cannot be effectively excited. Hence, the isolation between adjacent microstrip patch antennas is significantly improved without the need for additional decoupling structure. However, limited by the structure of the antenna, the weak field self-decoupling method is only applicable to the E-plane coupled MIMO microstrip patch antenna.

In summary, the decoupling structure designs mainly suffer from problems such as large array element spacing, a complex decoupling structure, and high profile. In this regard, a simple passive metal strip decoupling dielectric wall is designed in this paper to suppress the mutual coupling by cancelling the coupling effect of the original path when the MIMO antenna element spacing is 1 mm. Moreover, a pair of L-shaped parasitic resonant structures are introduced on the patch antenna feed line to improve its impedance matching bandwidth. The simulation and experimental results show that the MIMO antenna still has high isolation and good impedance matching bandwidth in the operating frequency band even when the array element spacing is very close. This decoupling structure can be effectively applied to MIMO antennas of different frequency bands and types.

II. ANTENNA DESIGN AND ANALYSIS

Fig. 1(a) displays the overall structure of the MIMO antenna and the basic structure of the passive metal strip decoupling dielectric wall. The proposed antenna was built on an FR4 substrate with a relative permittivity of $\varepsilon_r = 4.4$, a loss tangent of $\tan\delta = 0.02$ and a thickness h=1.0 mm. A $\lambda/2$ passive metal strip decoupling dielectric wall is embedded between two antenna elements with a spacing of only 1 mm.

The decoupled dielectric wall consists of half-wavelength microstrip lines on both sides of an FR4 substrate and two plugs at the bottom, as shown in Fig. 1(b). It should be noted that the plug is only used to fix the decoupling structure and does not affect the other performance of the antenna. Similarly, two plug slots are provided at the antenna dielectric substrate and the bottom so that the decoupling structure can be fixed on the antenna dielectric substrate, as shown in Fig. 1(c).
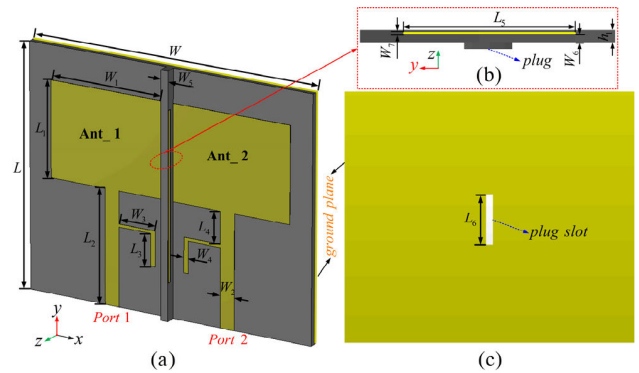

FIGURE 1. Proposed MIMO antenna structure. (a) Top, (b) passive metal strip decoupling dielectric wall, and (c) bottom. Detailed dimensions: W = 39 mm, W_1 = 16 mm, W_2 = 1.9 mm, W_3 = 5.0 mm, W_4 = 0.6 mm, W_5 = 1.0 mm, W_6 = 0.8 mm, W_7 = 0.4 mm, L = 32 mm, L_1 = 12.55 mm, L_2 = 14 mm, L_3 = 5.0 mm, L_4 = 4.25 mm, L_5 = 22 mm, L_6 = 7 mm, h_1 = 1.3 mm.

A. L-SHAPED PARASITIC STUBS

In general, to improve the impedance matching of the antenna, a method of loading a parasitic resonant structure can be adopted. Loading a resonant structure that is closer to the resonant mode of the patch antenna can enhance the resonant mode of the antenna, thereby improving its impedance characteristics to a certain extent.

Fig. 2 shows a comparison of the S-parameter values with and without loading the L-shaped parasitic resonance stub. When the resonant structure is not loaded, the reflection coefficient and mutual coupling of the MIMO antenna is unacceptable for the MIMO antenna system. Conversely, by loading the L-shaped parasitic resonance stub between two very closely spaced microstrip antennas, the original poor S_{11} of −7 dB can be improved to better than −15 dB at the resonant frequency of 5.37 GHz. In addition, it can be observed from the S_{21} curve that in the operating frequency band, loading the L-shaped parasitic stub has almost negligible impact on the isolation of the MIMO antenna.

B. DECOUPLING STRUCTURE DESIGN AND MECHANISM ANALYSIS

The decoupling mechanism of the current cancellation decoupling method is realized by utilizing additional coupling between antennas. To be specific, an indirect coupling field is added between antennas, which meets the requirement of approximate equalization in amplitude and opposite in phase between the original direct coupling field and the added indirect coupling field. At present, there are two main ways to increase the indirect coupling field, namely the
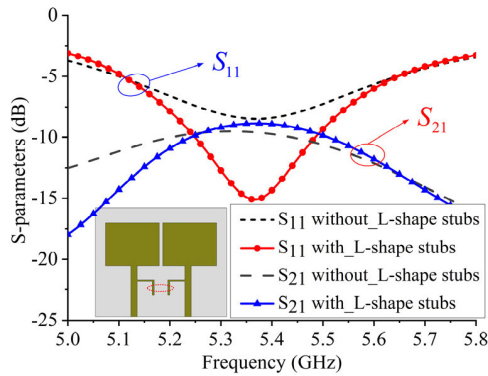
FIGURE 2. S-parameter of the MIMO antenna with and without the L-shaped parasitic resonance stubs.

non-connected type [11], [12], [13], [14], [15] and connected type [16], [17], [18].

Fig. 3 shows the voltage and current distribution of the $\lambda/2$ microstrip transmission line. When a $\lambda/2$ microstrip transmission line with both ends short-circuited is used for the resonator, the signal passing through it can have a 180° phase shift at the resonant frequency. Therefore, the current coupled to Ant_2 respectively through the $\lambda/2$ microstrip transmission line and Ant_1 satisfies the condition of equal amplitude and opposite phase. i.e.,

$$i = \begin{pmatrix} i_0 \\ -i_0 \end{pmatrix} \quad (1)$$
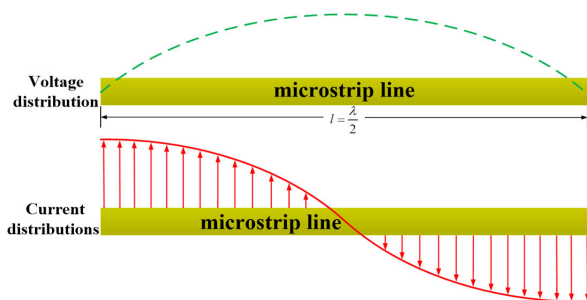
FIGURE 3. Voltage and current distribution of $\lambda/2$ microstrip transmission line.

To verify the correctness of the principle of field decoupling, the surface current distribution of the MIMO antenna with and without a decoupling structure at the center frequency of 5.37 GHz is simulated. The Port 1 is connected to the excitation source, and port 2 is connected to a 50 Ω load. It can be seen from Fig. 4(a) that in the absence of a decoupling structure, a surface current opposite to that of Ant_1 is induced on Ant_2, which is generated by the direct coupling field between the antenna elements. After adding the proposed decoupling structure, the passive metal strips on the structure will also be excited by Ant_1, and a surface current opposite to that of Ant_1 will appear, as shown in Fig. 4(b). Consequently, the current indirectly induced on Ant_2 through the passive metal strip is opposite to the current directly induced on Ant_2 through Ant_1, and the two can cancel each other, thereby reducing the current directly

coupled to Ant_2 from Ant_1. Finally, it can be clearly seen from Fig. 4(c) that after adding the decoupling structure, the intensity of the induced current on Ant_2 is weak, and its current direction is consistent with that on Ant_1. It further proves the effectiveness of the decoupling structure.
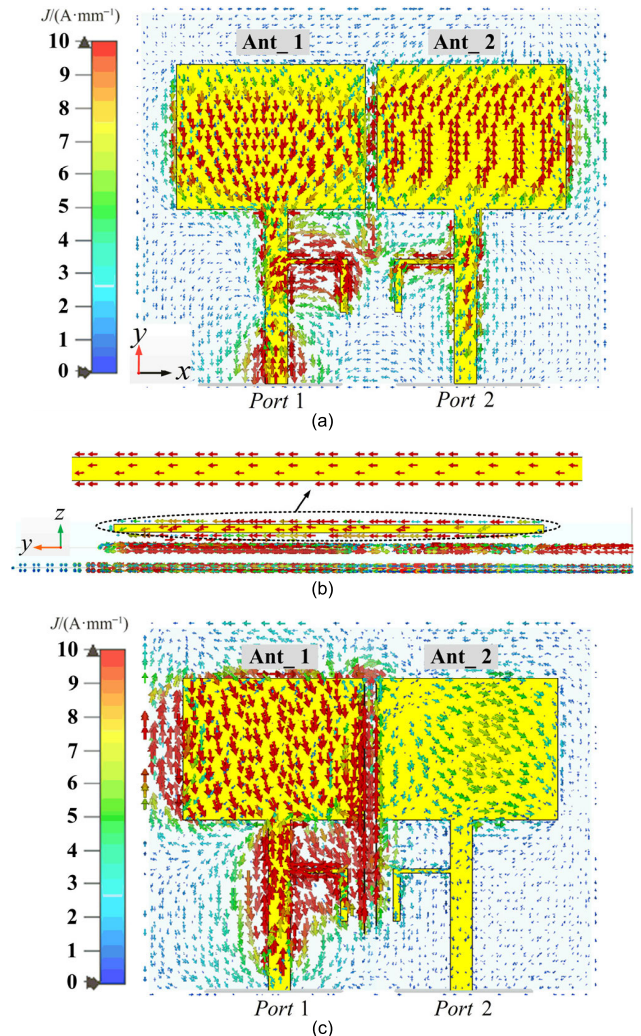

FIGURE 4. Current distributions at 5.37 GHz of the MIMO antenna: (a) without decoupling structure, (b) Current distribution on the $\lambda/2$ microstrip transmission line and (c) with decoupling structure.

Fig. 5 shows a comparison diagram of antenna S-parameters with and without a passive metal strip decoupling dielectric wall. When the decoupling dielectric wall is not loaded, the isolation of the antenna is only 8.5 dB, indicating that the coupling between the antennas is very strong. When the decoupling structure is added, the isolation of the MIMO antenna is significantly improved. The isolation at the resonant frequency is approximately 60 dB, achieving a coupling suppression of more than 51.5 dB. Further, with the addition of the decoupling structure, the S_{11} of the antenna improved from −15 dB to −33 dB, further verifying the effectiveness of the decoupling dielectric wall designed in this study.

Next, the influence of the relevant parameters of the L-shaped parasitic stub on the antenna performance is
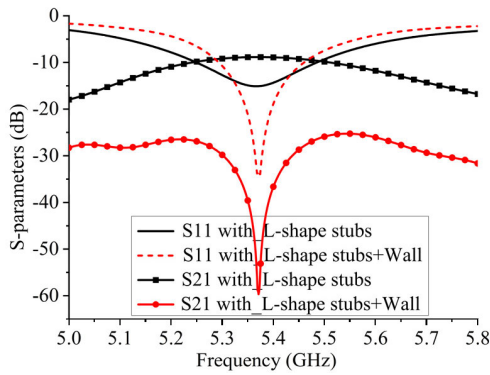
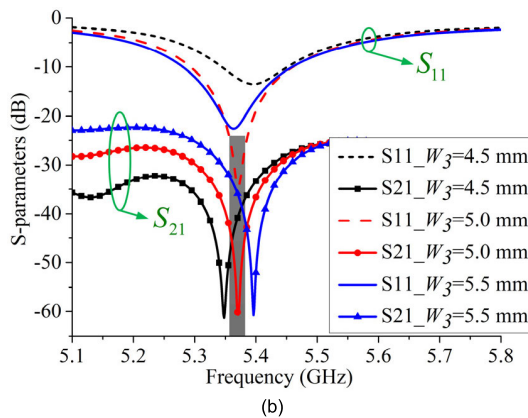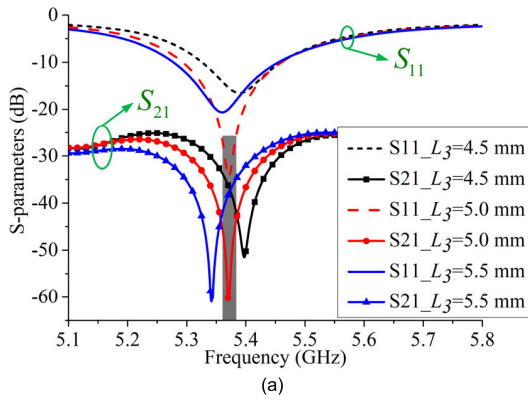**FIGURE 5.** S-parameter of the MIMO antenna with and without the decoupling structures.

(a)

(b)

FIGURE 6. Influence of different parameters on the antenna S-parameters. (a) L_3 and (b) W_3.

(a)

(b)

FIGURE 7. Influence of different parameters on the antenna S-parameters. (a) L_5 and (b) W_6.

Fig. 7 analyzes the influence of the length L_5 and height W_6 of the half-wavelength metal microstrip line on the decoupling dielectric wall on the isolation of the MIMO antenna. As can be seen from Fig. 7(a), the impedance matching and isolation of the MIMO antenna will vary with the length of the metal microstrip line, which indicates that only when the size of the metal microstrip line is within a reasonable range, can it be excited by Ant_1, resulting in resonance. Based on the above analysis, CST electromagnetic simulation software was used to optimize the relevant parameters, and the values of L_5 and W_6 were finally determined to be 22 mm and 5.8 mm, respectively.

III. RESULTS AND DISCUSSION
A. S-PARAMETERS
Fig. 8(a) presents the prototype of the fabricated antenna. To facilitate the assembly of the antenna and the decoupling structure, a plug with a width of 7 mm and a length of 1.0 mm are designed on the decoupling dielectric wall and mounting holes of the same size are reserved on the antenna, as shown in Fig. 8(b). The plug is then attached to the dielectric wall with insulating glue after installation.

The proposed antenna is simulated and measured using the full-wave simulation software CST, version 2021, and Keysight E5063A vector network analyzer, respectively. The simulated and measured reflection coefficients and isolation results are presented in Fig. 9. It can be seen that in the

analyzed. As can be seen from Fig. 6(a), by changing the length of L_3, the impedance matching of the antenna at the resonant frequency can be effectively controlled. Similarly, W_3 not only affects the length of the L-shaped resonant structure but also affects the mutual coupling cancellation between itself and the decoupling dielectric wall. Therefore, it is extremely crucial to select a reasonable value. Fig. 6(b) presents the results for a different value of W_3. The value of W_3 is selected to be approximately 5 mm, and the impedance matching of the MIMO antenna was approximately 33 dB. The isolation of the antenna was also observed to be the best in this setting ($|S_{21}| > 60$ dB @5.37 GHz). Therefore, it is finally determined that the values of L_3 and W_3 are both 5 mm.
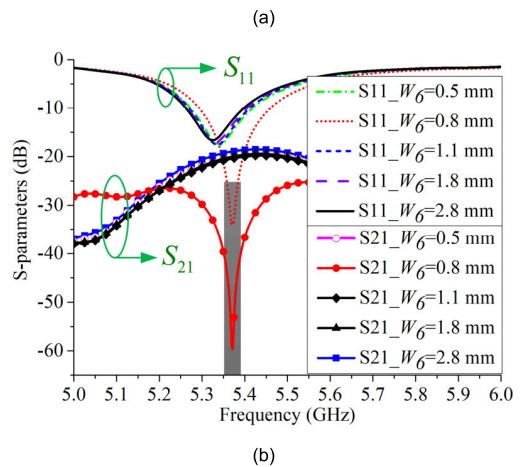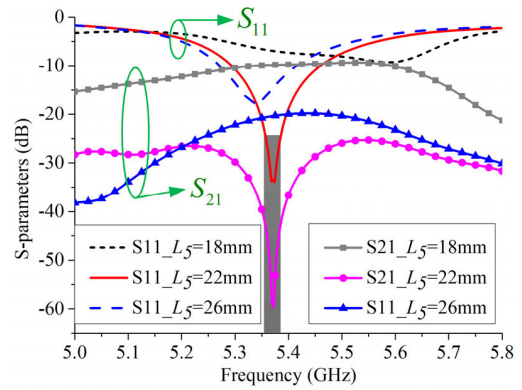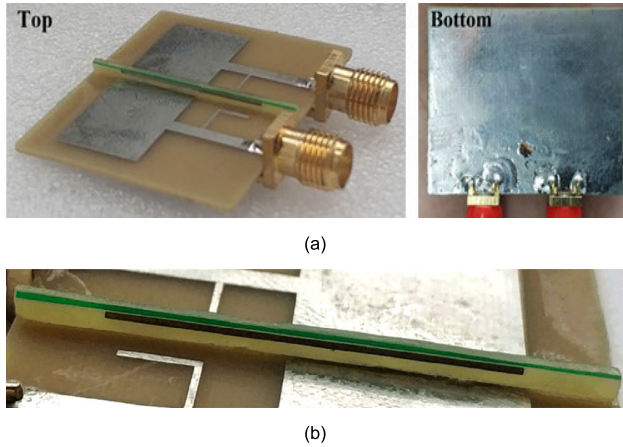
FIGURE 8. (a) Photograph of the MIMO antenna, (b) decoupling structure.
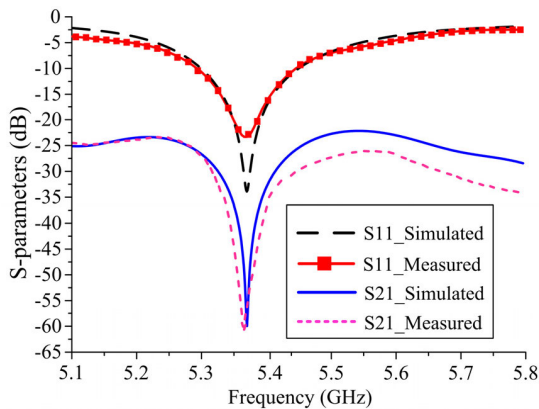
FIGURE 9. Simulated and measured S-parameters.

FIGURE 10. Simulated and measured radiation patterns of Ant_1 at 5.37 GHz. (a) E-plane, (b) H-plane.

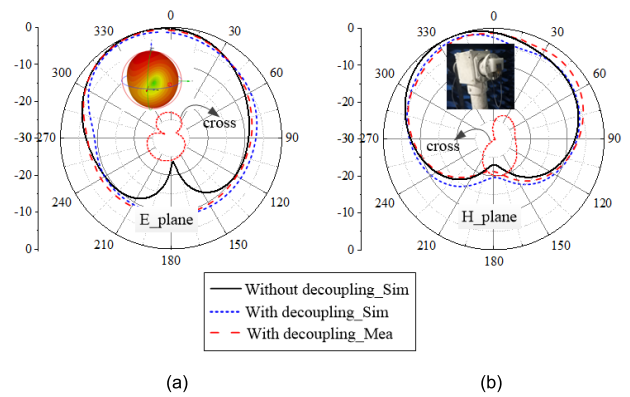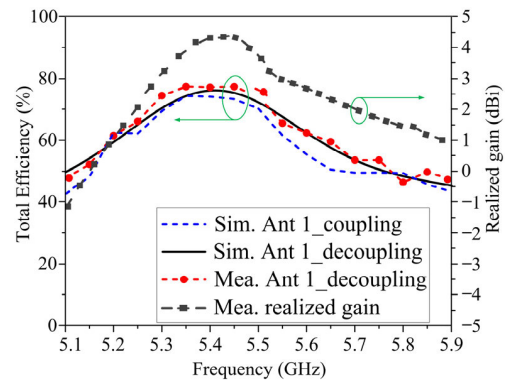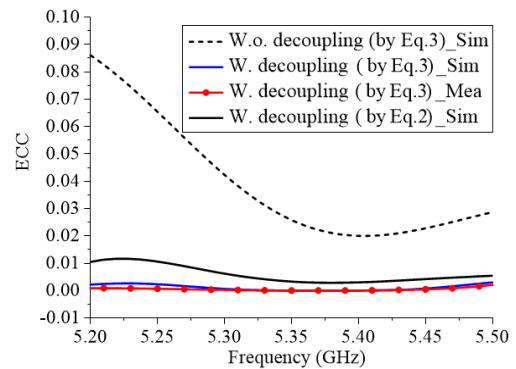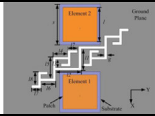FIGURE 11. Simulated and measured total efficiencies and realized gain of Ant_1.
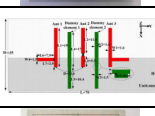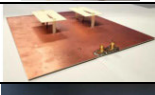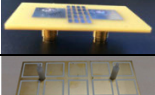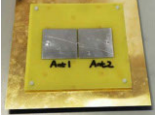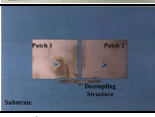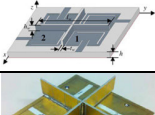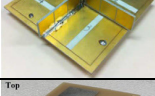
FIGURE 12. Simulated and measured ECC of the proposed MIMO antenna.

5.3−5.46 GHz operating frequency band, the isolation of the MIMO antenna is greater than 30 dB and the maximum value is 61 dB at the center frequency of 5.37 GHz. It should be emphasized that the antenna measurement and simulation results are in good agreement, which further illustrates the rationality of the design.

B. RADIATION CHARACTERISTICS

Fig. 10 displays the measured and simulated normalized pattern of the MIMO antenna at 5.37 GHz. The simulated and measured radiation patterns of the antenna are in good agreement, and the maximum measured realized gain of the antenna is about 4.54 dBi (Fig. 11), and the cross-polarization component in the boresight direction is low. However, compared with the radiation pattern without a decoupling structure, the introduction of a decoupling structure will enhance the antenna's backward radiation and increase the side lobes. This is mainly due to the fact that the field generated by the passive metal strip is similar to the traditional dipole radiation field. In addition to being able to offset the coupling field between the antennas, the decoupling structure will affect the radiation of the antenna. Further, we found that this phenomenon will be more obvious as the distance W_1 between the metal strip and ground on the decoupling structure increases. Therefore, while maintaining the other performance of the antenna, the height of the decoupling

structure should be reduced as much as possible to reduce the impact on radiation performance.

Since the structures of Ant_1 and Ant_2 are symmetrical to each other, only the total efficiency when Ant_1 is excited is plotted in Fig. 11. It can be seen that the simulated and measured total efficiency of the antenna in the operating bandwidth are 70.1%~74.8% and 74.4%~78.3%, respectively. The abovementioned results are basically consistent. In addition, the result of total efficiency of the antenna with and without decoupling are close in the operating bandwidth, which indicates that the metallic and dielectric loss introduced by the decoupling structure are relatively small.

TABLE 1. Performance comparison of the proposed method with previously reported methods.

Ref./Year	Antenna structure	Decoupling method	Operating bandwidth	Edge-to-edge spacing	Height of antenna MIMO	Maximal isolation improvement	Design complexity
[3]/2021		Mode cancellation method	5.73–5.9 GHz	7.5 mm ($0.145\lambda_0$)	2 mm ($0.039\lambda_0$)	46 dB	Low
[8]/2016		Fractal defected ground structure	2.28–2.325 GHz	20 mm ($0.13\lambda_0$)	3.18 mm ($0.024\lambda_0$)	39 dB	High
[11]/2019		Field cancellation method PS (non-connected type)	2.4–2.5 GHz /5.6–5.9 GHz	$\approx$ 2.2 mm ($\approx 0.117\lambda_0$)	0.8 mm ($0.0064\lambda_0$)	16 dB /19 dB	Low
[15]/2018		Field cancellation method PS (non-connected type)	3.475–3.57 GHz	12.6 mm ($0.147\lambda_0$)	0.8 mm ($0.009\lambda_0$)	42 dB	Low
[17]/2020		Field cancellation method NL (connected type)	2.37–2.71 GHz	2.2 mm ($0.018\lambda_0$)	0.76mm ($0.006\lambda_0$)	12 dB	High
[19]/2021		Field cancellation method DN (connected type)	2.3–2.4 GHz	25 mm ($0.197\lambda_0$)	22.76 mm ($0.178\lambda_0$)	21 dB	High
[23]/2017		Polarization-conversion isolators	5.7–6.0 GHz	9 mm ($0.174\lambda_0$)	1.6 mm ($0.03\lambda_0$)	22.3 dB	High
[26]/2019		Slot metasurface	3.53–3.57 GHz	2 mm ($0.023\lambda_0$)	16.53 mm ($0.19\lambda_0$)	41 dB	High
[29]/2022		FSS wall	3.4–3.6 GHz	16 mm ($0.189\lambda_0$)	28 mm ($0.32\lambda_0$)	15 dB	High
[36]/2021		Mode cancellation method	2.38–2.51 GHz	2 mm ($0.016\lambda_0$)	5 mm ($0.04\lambda_0$)	10.4 dB	Low
[37]/2021		Phase shift	3.125–3.18 GHz	2.6 mm ($0.027\lambda_0$)	2.0 mm ($0.02\lambda_0$)	11 dB	Low
[38]/2018		Orthogonally decoupling dielectric wall	3.47–3.53 GHz /5.68–5.72 GHz	2 mm ($0.023\lambda_0$)	3.96 mm ($0.046\lambda_0$)	10.8 dB /15.6 dB	Low
[39]/2015		Orthogonally decoupling dielectric wall	2.396–2.45 GHz	5.4 mm ($0.043\lambda_0$)	21.6 mm ($0.17\lambda_0$)	35 dB	High
This work		Current cancellation method (non-connected type)	5.3–5.46 GHz	1 mm ($0.017\lambda_0$)	2.9 mm ($0.05\lambda_0$)	51.5 dB	Low

NL: Neutralization lines, DN: Decoupling networks, PS: Parasitic decoupling structure

The above results present that the coupling between MIMO antenna elements can be effectively reduced without the radiation efficiency being affected.

C. DIVERSITY PERFORMANCE

To obtain a result similar to an actual environment, a more complicated formula, i.e., (2), is used to calculate the ECC

of the MIMO antenna [29]. As the laboratory equipment does not support currently the test of 3D radiation patterns, the ECC curve shown in Fig. 10 is the result calculated using (3). It should be noted that the premise of using (3) is that the antenna has a higher radiation efficiency. As shown in Fig. 12, the proposed MIMO antenna has a very low ECC (ECC<0.003) in the operating frequency band, and the

measured and simulated results are basically the same.

$$\rho_{eij} = \frac{\left| \iint_{4\pi} \left[F_{Ant\_i}(\theta, \varphi) \cdot F_{Ant\_j}(\theta, \varphi) \right] d\Omega \right|^2}{\iint_{4\pi} \left| F_{Ant\_i}(\theta, \varphi) \right|^2 d\Omega \iint_{4\pi} \left| F_{Ant\_j}(\theta, \varphi) \right|^2 d\Omega} \tag{2}$$

$$\rho_{eij} = \frac{\left| S_{11}^* S_{12} + S_{21}^* S_{22} \right|^2}{\left(1 - |S_{11}|^2 - |S_{21}|^2 \right) \left(1 - |S_{22}|^2 - |S_{12}|^2 \right)} \tag{3}$$

In (2), i and j denote the number of antenna elements, F_{Ant_i} denotes the 3-D far-field radiation patterns.

Finally, to highlight the advantages of the proposed MIMO antenna, Table 1 presents the related research work that has been reported in the field of MIMO antenna coupling suppression technology. Compared with References [3], [8], [15], [19], [23], [29], and [37], the edge-to-edge distance between the proposed MIMO antenna elements is smaller and the isolation is greater. However, the profile height of the antenna proposed in this paper is slightly higher than that of the antenna in references [3], [11], [15], [17], and [37]. Although relatively novel weak field coupling self-decoupling method was adopted in [31], it is more difficult to implement than traditional methods, and there are no system design guidelines currently. In addition, orthogonal decoupling dielectric walls are designed as metasurfaces or more complex structures, which mainly suppress spatially coupled waves [38], [39]. First, the overall size of the antenna increases owing to the bulky metasurface decoupling dielectric wall, which is not suitable for the miniaturization design with regards to the proposed antenna. Whilst secondly, the position and height of designed metasurfaces have a significant impact on the mutual coupling so that optimization is essential in the design process.

In summary, it can be seen that the decoupling design of the parasitic structure proposed in this paper is simpler than that of the MIMO antenna using the neutralization line and the decoupling network. The decoupling effect is better when antenna elements are very closely arranged. Compared with the planar parasitic structure, the decoupling structure proposed in this paper still shows good coupling suppression ability.

IV. CONCLUSION

A compact two-element MIMO antenna with high isolation is designed in this study. To enhance the isolation, a simple decoupling dielectric wall is inserted between the antenna elements. In addition, a pair of L-shaped parasitic resonance stubs is loaded on the feeding microstrip line, which significantly improves the impedance matching of the antenna. The experimental and simulation results are in good agreement, and the advantages of this design are further highlighted by comparing with the published research. In addition, the study shows that the method can be generalized to other types of printed antennas with general applicability.

REFERENCES

[1] J. G. Andrews, S. Buzzi, W. Choi, S. V. Hanly, A. Lozano, A. C. K. Soong, and J. C. Zhang, "What will 5G be?" *IEEE J. Sel. Areas Commun.*, vol. 32, no. 6, pp. 1065–1082, Jun. 2014, doi: 10.1109/JSAC.2014.2328098.

[2] L. Sun, Y. Li, Z. Zhang, and H. Wang, "Self-decoupled MIMO antenna pair with shared radiator for 5G smartphones," *IEEE Trans. Antennas Propag.*, vol. 68, no. 5, pp. 3423–3432, May 2020, doi: 10.1109/TAP.2019.2963664.

[3] Q. X. Lai, Y. M. Pan, S. Y. Zheng, and W. J. Yang, "Mutual coupling reduction in MIMO microstrip patch array using TM$_{10}$ and TM$_{02}$ modes," *IEEE Trans. Antennas Propag.*, vol. 69, no. 11, pp. 7562–7571, Nov. 2021, doi: 10.1109/TAP.2021.3090520.

[4] Y.-M. Zhang and S. Zhang, "A side-loaded-metal decoupling method for 2×N patch antenna arrays," *IEEE Antennas Wireless Propag. Lett.*, vol. 20, no. 5, pp. 668–672, May 2021, doi: 10.1109/LAWP.2021.3059736.

[5] M. Sharawi, *Printed MIMO Antenna Engineering*. Norwood, MA, USA: Artech House, 2014.

[6] B. Qian, X. Chen, and A. Kishk, "Decoupling of microstrip antennas with defected ground structure using the common/differential mode theory," *IEEE Antennas Wireless Propag. Lett.*, vol. 20, no. 5, pp. 828–832, May 2021, doi: 10.1109/LAWP.2021.3064972.

[7] D. Gao, Z.-X. Cao, S.-D. Fu, X. Quan, and P. Chen, "A novel slot-array defected ground structure for decoupling microstrip antenna array," *IEEE Trans. Antennas Propag.*, vol. 68, no. 10, pp. 7027–7038, Oct. 2020, doi: 10.1109/TAP.2020.2992881.

[8] K. Wei, J.-Y. Li, L. Wang, Z.-J. Xing, and R. Xu, "Mutual coupling reduction by novel fractal defected ground structure bandgap filter," *IEEE Trans. Antennas Propag.*, vol. 64, no. 10, pp. 4328–4335, Oct. 2016, doi: 10.1109/TAP.2016.2591058.

[9] A. Khan, S. Bashir, S. Ghafoor, and K. K. Qureshi, "Mutual coupling reduction using ground stub and EBG in a compact wideband MIMO-antenna," *IEEE Access*, vol. 9, pp. 40972–40979, 2021, doi: 10.1109/ACCESS.2021.3065441.

[10] X. Tan, W. Wang, Y. Wu, Y. Liu, and A. A. Kishk, "Enhancing isolation in dual-band meander-line multiple antenna by employing split EBG structure," *IEEE Trans. Antennas Propag.*, vol. 67, no. 4, pp. 2769–2774, Apr. 2019, doi: 10.1109/TAP.2019.2897489.

[11] X. Shen, F. Liu, L. Zhao, G.-L. Huang, X. Shi, Q. Huang, and A. Chen, "Decoupling of two strongly coupled dual-band antennas with reactively loaded dummy element array," *IEEE Access*, vol. 7, pp. 154672–154682, 2019, doi: 10.1109/ACCESS.2019.2948897.

[12] A. A. Ghannad, M. Khalily, P. Xiao, R. Tafazolli, and A. A. Kishk, "Enhanced matching and vialess decoupling of nearby patch antennas for MIMO system," *IEEE Antennas Wireless Propag. Lett.*, vol. 18, no. 6, pp. 1066–1070, Jun. 2019, doi: 10.1109/LAWP.2019.2906308.

[13] S. Farsi, H. Aliakbarian, D. Schreurs, B. Nauwelaers, and G. A. E. Van denbosch, "Mutual coupling reduction between planar antennas by using a simple microstrip U-section," *IEEE Antennas Wireless Propag. Lett.*, vol. 11, pp. 1501–1503, 2012, doi: 10.1109/LAWP.2012.2232274.

[14] J.-N. Hwang and S.-J. Chung, "Isolation enhancement between two packed antennas with coupling element," *IEEE Antennas Wireless Propag. Lett.*, vol. 10, pp. 1263–1266, 2011, doi: 10.1109/LAWP.2011.2174957.

[15] J.-Y. Deng, J.-Y. Li, and L.-X. Guo, "Decoupling of a three-port MIMO antenna with different impedances using reactively loaded dummy elements," *IEEE Antennas Wireless Propag. Lett.*, vol. 17, no. 3, pp. 430–433, Mar. 2018, doi: 10.1109/LAWP.2018.2793939.

[16] S. Zhang and G. F. Pedersen, "Mutual coupling reduction for UWB MIMO antennas with a wideband neutralization line," *IEEE Antennas Wireless Propag. Lett.*, vol. 15, pp. 166–169, 2016, doi: 10.1109/LAWP.2015.2435992.

[17] M. Li, L. Jiang, and K. L. Yeung, "A general and systematic method to design neutralization lines for isolation enhancement in MIMO antenna arrays," *IEEE Trans. Veh. Technol.*, vol. 69, no. 6, pp. 6242–6253, Jun. 2020, doi: 10.1109/TVT.2020.2984044.

[18] Y. Wang and Z. Du, "A wideband printed dual-antenna with three neutralization lines for mobile terminals," *IEEE Trans. Antennas Propag.*, vol. 62, no. 3, pp. 1495–1500, Mar. 2014, doi: 10.1109/TAP.2013.2295226.

[19] M. Li, M. Wang, L. Jiang, and K. L. Yeung, "Decoupling of antennas with adjacent frequency bands using cascaded decoupling network," *IEEE Trans. Antennas Propag.*, vol. 69, no. 2, pp. 1173–1178, Feb. 2021, doi: 10.1109/TAP.2020.3010956.

[20] Y.-F. Cheng and K.-K.-M. Cheng, "Compact wideband decoupling and matching network design for dual-antenna array," *IEEE Antennas Wireless Propag. Lett.*, vol. 19, no. 5, pp. 791–795, May 2020, doi: 10.1109/LAWP.2020.2980293.

[21] M. Li, L. Jiang, and K. L. Yeung, "A novel wideband decoupling network for two antennas based on the Wilkinson power divider," *IEEE Trans. Antennas Propag.*, vol. 68, no. 7, pp. 5082–5094, Jul. 2020, doi: 10.1109/TAP.2020.2981679.

[22] K. Wei, J. Li, L. Wang, and R. Xu, "Microstrip antenna array mutual coupling suppression using coupled polarisation transformer," *IET Microw., Antennas Propag.*, vol. 11, no. 13, pp. 1836–1840, Oct. 2017, doi: 10.1049/iet-map.2016.1154.

[23] Y.-F. Cheng, X. Ding, W. Shao, and B.-Z. Wang, "Reduction of mutual coupling between patch antennas using a polarization-conversion isolator," *IEEE Antennas Wireless Propag. Lett.*, vol. 16, pp. 1257–1260, 2016, doi: 10.1109/LAWP.2016.2631621.

[24] Z. Wang, C. Li, Q. Wu, and Y. Yin, "A metasurface-based low-profile array decoupling technology to enhance isolation in MIMO antenna systems," *IEEE Access*, vol. 8, pp. 125565–125575, 2020, doi: 10.1109/ACCESS.2020.3007188.

[25] F. Liu, J. Guo, L. Zhao, G.-L. Huang, Y. Li, and Y. Yin, "Dual-band metasurface-based decoupling method for two closely packed dual-band antennas," *IEEE Trans. Antennas Propag.*, vol. 68, no. 1, pp. 552–557, Jan. 2020, doi: 10.1109/TAP.2019.2940316.

[26] H. Luan, C. Chen, W. Chen, L. Zhou, H. Zhang, and Z. Zhang, "Mutual coupling reduction of closely E/H-plane coupled antennas through metasurfaces," *IEEE Antennas Wireless Propag. Lett.*, vol. 18, no. 10, pp. 1996–2000, Oct. 2019, doi: 10.1109/LAWP.2019.2936096.

[27] F. Liu, J. Guo, L. Zhao, X. Shen, and Y. Yin, "A meta-surface decoupling method for two linear polarized antenna array in sub-6 GHz base station applications," *IEEE Access*, vol. 7, pp. 2759–2768, 2018, doi: 10.1109/ACCESS.2018.2886641.

[28] A. Jafargholi, A. Jafargholi, and H. J. Choi, "Mutual coupling reduction in an array of patch antennas using CLL metamaterial superstrate for MIMO applications," *IEEE Trans. Antennas Propag.*, vol. 67, no. 1, pp. 179–189, Jan. 2019, doi: 10.1109/TAP.2018.2874747.

[29] F. Merzaki, P. Besnier, M. Himdi, X. Castel, M. Sergolle, T. Levavasseur, and P. Caldamone, "A compact double-sided FSS absorbing wall for decoupling 5G antenna arrays," *IEEE Trans. Electromagn. Compat.*, vol. 64, no. 2, pp. 303–314, Apr. 2022, doi: 10.1109/TEMC.2021.3129368.

[30] M. Rezapour, M. Rashed, and A. Jalil, "Isolation enhancement of rectangular dielectric resonator antennas using wideband double slit complementary split ring resonators," *Int. J. RF Microw. Comput.-Aided Eng.*, vol. 29, no. 7, pp. 1–11, 2019, doi: 10.1002/mmce.21746.

[31] H. Lin, Q. Chen, Y. Ji, X. Yang, J. Wang, and L. Ge, "Weak-field-based self-decoupling patch antennas," *IEEE Trans. Antennas Propag.*, vol. 68, no. 6, pp. 4208–4217, Jun. 2020, doi: 10.1109/TAP.2020.2970109.

[32] J. Sui and K. L. Wu, "A self-decoupled antenna array using inductive and capacitive couplings cancellation," *IEEE Trans. Antennas Propag.*, vol. 68, no. 7, pp. 5289–5296, Jul. 2020, doi: 10.1109/TAP.2020.2977823.

[33] Y. M. Pan, Y. Hu, and S. Y. Zheng, "Design of low mutual coupling dielectric resonator antennas without using extra decoupling element," *IEEE Trans. Antennas Propag.*, vol. 69, no. 11, pp. 7377–7385, Nov. 2021, doi: 10.1109/TAP.2021.3090807.

[34] L. Sun, Y. Li, Z. Zhang, and H. Wang, "Antenna decoupling by common and differential modes cancellation," *IEEE Trans. Antennas Propag.*, vol. 69, no. 2, pp. 672–682, Feb. 2021, doi: 10.1109/TAP.2020.3009427.

[35] K.-L. Wong, M.-F. Jian, C.-J. Chen, and J.-Z. Chen, "Two-port same-polarized patch antenna based on two out-of-phase TM_{10} modes for access-point MIMO antenna application," *IEEE Antennas Wireless Propag. Lett.*, vol. 20, no. 4, pp. 572–576, Apr. 2021, doi: 10.1109/LAWP.2021.3057420.

[36] L. Sun, Y. Li, and Z. Zhang, "Decoupling between extremely closely spaced patch antennas by mode cancellation method," *IEEE Trans. Antennas Propag.*, vol. 69, no. 6, pp. 3074–3083, Jun. 2021, doi: 10.1109/TAP.2020.3030922.

[37] T. Pei, L. Zhu, J. Wang, and W. Wu, "A low-profile decoupling structure for mutual coupling suppression in MIMO patch antenna," *IEEE Trans. Antennas Propag.*, vol. 69, no. 10, pp. 6145–6153, Oct. 2021, doi: 10.1109/TAP.2021.3098565.

[38] A. Boukarkar, X. Q. Lin, Y. Jiang, L. Y. Nie, P. Mei, and Y. Yu, "A miniaturized extremely close-spaced four-element dual-band MIMO antenna system with polarization and pattern diversity," *IEEE Antennas Wireless Propag. Lett.*, vol. 17, no. 1, pp. 134–137, Jan. 2018, doi: 10.1109/LAWP.2017.2777839.

[39] G. Zhai, Z. N. Chen, and X. Qing, "Enhanced isolation of a closely spaced four-element MIMO antenna system using metamaterial mushroom," *IEEE Trans. Antennas Propag.*, vol. 63, no. 8, pp. 3362–3370, Aug. 2015, doi: 10.1109/TAP.2015.2434403.

ZHONGHONG DU was born in Tianshui, Gansu, China, in 1994. He received the B.S. degree in electronic information and the M.S. degree in communicating engineering from the Xi'an University of Technology, Xi'an, China, in 2017 and 2020, respectively, where he is currently pursuing the Ph.D. degree in electromagnetic field and microwave technology. His research interests include MIMO antennas decoupling technology, electromagnetic metasurface, and RF circuits.

He serves as a Reviewer for the IEEE ANTENNAS AND WIRELESS PROPAGATION LETTERS and *International Journal of Microwave and Wireless Technologies*.

XIAOHUI ZHANG received the B.S. degree in industrial automation, the M.S. degree in control science and engineering, and the Ph.D. degree in control science and engineering from the Xi'an University of Technology, Xi'an, China, in 1995, 2002, and 2009, respectively. He is currently a Professor with the Information and Control Department, Xi'an University of Technology. His recent research interests include advanced navigation, signal processing and pattern recognition, electromagnetic technology, and antenna design.

PEIYU QIN received the B.S. degree in information engineering from Tianjin Normal University, Tianjin, China, in 2019. She is currently pursuing the graduate degree with the Xi'an University of Technology, Xi'an, China. Currently, she is engaged in research on MIMO antenna coupling suppression and polarization rotation isolation structure with the Department of Electronic and Electrical Engineering, Brunel University, London, U.K.

YURONG PU (Member, IEEE) received the B.S., M.S., and Ph.D. degrees in electronic engineering from the Xi'an University of Technology, Xi'an, China, in 2004, 2007, and 2013, respectively.

She is currently an Associate Professor with the Department of Electronic Engineering, Xi'an University of Technology. Her current research interests include computational electromagnetics and wave propagation.
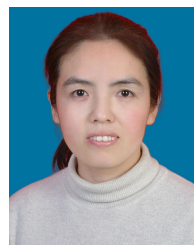
XIAOLI XI (Member, IEEE) received the B.S. degree in applied physics from the University of Defense Technology, Changsha, China, in 1990, the M.S. degree in biomedical engineering from Fourth Military Medical University, Xi'an, China, in 1998, and the Ph.D. degree in electrical engineering from Xi'an Jiaotong University, Xi'an, in 2004.

She is currently a Professor with the Electronics Engineering Department, Xi'an University of Technology, Xi'an. Her current research interests include wave propagation, antenna design, and communication signals processing. She serves as a reviewer for the IEEE TRANSACTIONS ON ANTENNAS AND PROPAGATION, IEEE ACCESS, and IEEE ANTENNAS AND WIRELESS PROPAGATION LETTERS.

• • •